

# Optimizing Hydrogel Production with Additive Manufacturing Techniques

Colin Fried, Rafee Akand, Sabrina Nilufar

Department of Mechanical Engineering  
Southern Illinois University Carbondale, 62901  
July 14, 2023

## Abstract

Additive manufacturing (AM) has become paramount in the quest for fast, affordable, individualized production. In the relatively short time that AM has been available, there have been great advances in many subsets of engineering and science. In particular, AM has provided new avenues for exploring biological systems due to its inherent ability to effectively produce complex geometries with novel materials. In fact, AM allows for the use of such novel materials that there is still very little known about the characteristics that many of these materials possess. To continue pushing boundaries, it is necessary to characterize these novel materials, which ultimately produces a great deal of waste. We have identified a novel polyacrylamide (PAA) resin that can be used with digital light processing (DLP) technologies to effectively produce biocompatible hydrogels. There are many deep implications to furthering the production of these hydrogels in fields like mechanosensing, drug-delivery, and cancer therapies, but it comes high economic and environmental costs. We have identified two potential methods for reducing the burden of producing these hydrogels: reusing the resin required for printing and reducing concentrations of the active ingredients within the resin itself. We have found that both of these avenues present much promise for the future of AM, biomaterials, and rheology.

# 1 Introduction

As additive manufacturing (AM) continues to progress, our goal is to help push our growing community into new frontiers. Biomaterials have been notoriously challenging to produce [protick], but our growing understanding of printing techniques, including fused deposition modeling (FDM) [chia, wasti], direct-ink writing, [mondal, simon] and stereolithography (SLA) [wasti, chia], has provided new insights for improving biomaterial production. In particular, SLA has become paramount in this process due to its ability to produce soft materials both quickly and uniformly [protick]. As we continue to make strides in material characterization and printing optimization, we can make progress in areas of research like cancer therapy [salmoria], drug delivery [md2020], and wearable devices [liu]. Furthermore, AM allows us to optimize production by allowing for individualized tuning due to its quick production time [horst], allowing for personalized products and potentially lower user-associated failure rates.

Stereolithography (SLA) is the oldest form of additive manufacturing, though it is still incredibly relevant in today's world [huang]. The process requires a photosensitive resin, which comes into contact with UV-light concentrated in a laser beam. The light follows a path in accordance with a sliced CAD file, which allows for layer-by-layer polymerization of the final product [huang, formlabs]. One derivative of SLA is called Digital Light Processing (DLP) — the only difference being that instead of guiding a laser, DLP shines the UV light all at once, simultaneously polymerizing each layer, allowing for XY resolutions as low as 35 microns [huang, formlabs]. DLP has shown exceptional promise in its inherent versatility — the resins can be tuned by the user, allowing for customizations that include biomaterial production [wasti, chia].

To fully actualize printing potential, it is necessary to characterize the behavior of printed materials under specific stimuli. An important avenue of biomaterial characterization hinges on mechanosensing studies [protick]. The transduction of mechanical stimuli into neural signals is an essential aspect of biomaterials, which has been related to areas of research including cell fate determination [kumar2017] and cancer behavior [broders]. These studies, among many others [tajik, kumar, wen, solon], have utilized soft polymers called *hydrogels* to understand the behavior of cells on a flexible substrate. In particular, polyacrylamide (PAA) has shown promise as being an effective material for hydrogel production [protick]. However, Protick et al. postulate that traditional hydrogels possess purely elastic mechanical characteristics, which may exhibit physiologically incompatible properties [protick]. Furthermore, it is shown that DLP-produced PAA hydrogels do not suffer from those same shortcomings, as they exhibit viscoelastic properties, which are compatible with living tissue [protick]. In addition, Protick et al. showcase a variety of DLP-resin recipes, showing that we can tune the hydrogels specifically to mimic different types of living tissue [protick].

The implications of tuning resin properties is paramount in hydrogel production and the greater field of biomaterials. However, it comes with a caveat – the PAA resin required for these biocompatible hydrogels is very expensive. Protick et al. present three different recipes, but we will focus on the recipe that produces a so-called *intermediate* stiffness profile due to its versatility in biocompatible hydrogel production [protick]. To achieve this profile, 10% v/v acrylamide, 0.3% v/v bis-acrylamide, and 2% v/v photoinitiator are mixed with type-III water [protick]. As a result, the resin is very expensive, and it quickly becomes difficult to make large batches of prints. We have identified the cost of resin to be a severe bottleneck in effectively scaling hydrogel production for both research and commercial purposes.

At this point in time, there are no tested alternatives to the monomer, cross-linker, and photoinitiator combination used for this PAA resin. However, there has been previous success with reusing polyethylene glycol resins [pyteraf], which opens up another potential avenue for reducing resin waste. To test this claim with PAA resin, we will print hydrogels comprised of differing layer heights such that we reuse the same resin three times for each respective layer height. In conjunction, we will test single prints of a resin batch containing 1.5% v/v photoinitiator to expand our understanding of resin composition and potential ingredient reduction. Following, we will test their respective rheological properties to see how much variation there is between prints as well as the impact of photoinitiator concentration on print viability. If there is little deviation from the first print with pristine resin, then recycling resin will be a viable option. Likewise, if lowered photoinitiator concentration results in little deviation from the 2% v/v control concentration, then

we will have found a parameter in resin production that has little impact on print quality. These findings may, in turn, significantly reduce resin cost with respect to DLP-produced PAA-hydrogels, ultimately optimizing further research and production.

## 2 Methods

### 2.1 Hydrogel Preparation

We followed the guidelines set by Protick et al. for producing *intermediate-hydrogels* [protick]. The hydrogels are printed from a resin comprised of 10% v/v acrylamide (monomer, Bio-Rad), 0.3% v/v bisacrylamide (cross-linker, Bio-Rad), type-III water, and lithium pheny-2,4,6-trimethylbenzoylphosphinate a.k.a. TPO-Li (photoinitiator, Colorado Photopolymer Solutions). For the consecutive prints, the concentration of TPO-Li was 2% v/v. For the photoinitiator concentration tests we compared the control concentration (2% v/v TPO-Li) with a lower TPO-Li concentration of 1.5% v/v. The resin was stored in an opaque container to prevent any premature polymerization.

The prints were made such that they adhered to a glass slide so we could easily remove them. To do so, we followed Protick et al. in their approach to printing the slides on a glass surface [protick]. The slides were coated in 3-aminopropylmethoxysilane (97%, Sigma-Aldrich) and left for 15 minutes. Following, the slides were submerged in type-III water for 10 minutes while being stirred before being baked in an oven for 1 hour at 160°C. Finally, the slides were coated in 0.5% glutaraldehyde (Grade II, Sigma-Aldrich) and stored at room temperature.

All of the printing was performed on a Phrozen Sonic Mini Resin 3D Printer. For both consecutive print testing and photoinitiator-concentration testing, the prints were cylindrical with 21 mm diameter and 2 mm total height. The hydrogels were printed with three distinct layer heights: 30 microns, 90 microns, and 150 microns. The 30 micron prints contained 8 base layers, the 90 micron prints contained 3 base layers, and the 150 micron prints contained 2 base layers. All of the respective base layers were exposed to UV-light for 50 seconds, while all of the other layers were exposed to UV-light for 6 seconds. At least three samples were made for each category of print to ensure reproducibility between samples. Following the printing process, the hydrogels were kept intact on the glass slides, submerged in phosphate-buffered saline (PBS) and refrigerated at 4°C for at least 12 hours to ensure saturation prior to rheological testing.

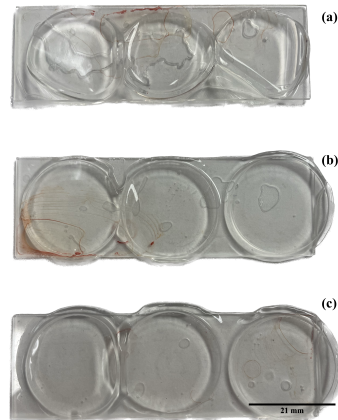


Figure 1: Hydrogels after 12-hour hydration in PBS: (a) 30 microns, (b) 90 microns, (c) 150 microns (no visible variation between prints or photoinitiator concentrations)



Figure 2: Thermo Scientific Haake Mars SAOS Rheometer

## 2.2 Rheological Testing

The rheological tests were performed on a Thermo Scientific Haake Mars Rheometer 2. The small angle oscillatory shear (saos) rheometer performed frequency sweeps on all of the samples from 0.01 Hz to 10 Hz, with 5 datapoints per decade. The frequency sweep test allowed us to measure the stiffness profile of the respective samples, providing us with how effectively a material stores energy (storage modulus), how effectively a material dissipates energy (loss modulus), and the ratio of loss modulus to storage modulus ( $\tan \delta$ ) [chen]. As  $\tan \delta$  becomes larger, so does the viscous nature of the material and its liquid-like behavior [chen]. Likewise, as  $\tan \delta$  approaches zero, the elastic nature of the material increases, presenting spring-like behavior [chen]. Protick et al. explain that living tissues generally exhibit viscoelastic properties, with  $0.1 \leq \tan \delta \leq 0.2$  [protick], which will act as guidelines for our results. The tests were performed at room temperature, with the hydrogels open to atmospheric conditions. When necessary, the gels were carefully cut to fit the measuring surface of the rheometer — this was variable, and depended on the degree of swelling within each respective gel.

## 3 Results and Discussion

### 3.1 Consecutive Prints

To identify the viscoelastic properties of the hydrogels, we focused on three low-frequency regions to closely resemble biological tissue [lacoste, cheng, soetens, erisken]:  $f = 0.01$  Hz (Fig. 3),  $f = 0.1$  Hz (Fig. 4), and  $f = 1$  Hz (Fig. 5). Within print 1 (control), we see a decrease in storage modulus with increasing layer height, implying the viscous nature of the hydrogel grows with decreasing accuracy in the print layers [favero]. There is a possibility of the hydrogels not fully polymerizing during the printing process, which would give rise to their increasingly viscous nature as the respective print detail. This trend will act as a guide for comparison between prints for the duration of our work, though it should be studied in greater detail for future work.

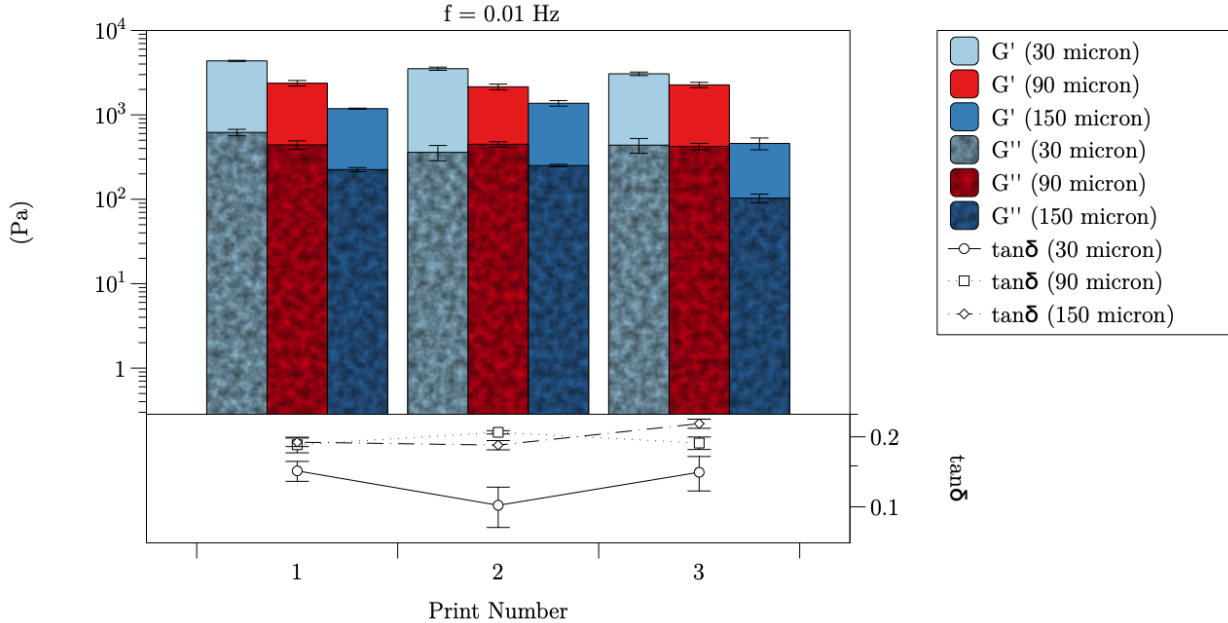


Figure 3: Primary axis: Storage Modulus at  $f = 0.01$  Hz with respect to print number for 30 micron, 90 micron, and 150 micron layer heights

Secondary axis:  $\tan \delta$  at  $f = 0.01$  Hz with respect to print number for 30 micron, 90 micron, and 150 micron layer heights

At  $f = 0.01$  Hz (3), there is noticeable variation between prints with 30 micron layer height. The second print presents a 19% difference in storage modulus with respect to the first print, coupled with a 28% difference in  $\tan \delta$ . These discrepancies continue to grow with print 3, additionally exhibiting nonlinear changes, implying that 30 micron hydrogels should always be printed with new resin. In contrast, there is considerably less variation within the 90 micron prints. The storage modulus varies with less than a 10% difference with respect to print 1 for the second iteration, and less than a 5% difference with respect to print 1 for the third iteration. However, the  $\tan \delta$  for print 2 has a 13% difference with respect to print 1. Although this difference decreases significantly at print 3, we see similar nonlinear activity resulting from the 90 micron prints as we did with the 30 micron prints. Finally, there is a 16% difference in storage modulus of the 150 micron print 2 data with respect to print 1, coupled with a 3% difference in  $\tan \delta$ . The small change in  $\tan \delta$  signifies the loss modulus is changing proportionally to the storage modulus, allowing for little change in the viscoelastic response within the hydrogel. To confirm this phenomenon, it is important to continue testing. However, there is little need to look at third iterations of resin for 150 micron prints, as the difference with respect to print 1 for both storage modulus and  $\tan \delta$  are too large to show any worthwhile similarities.

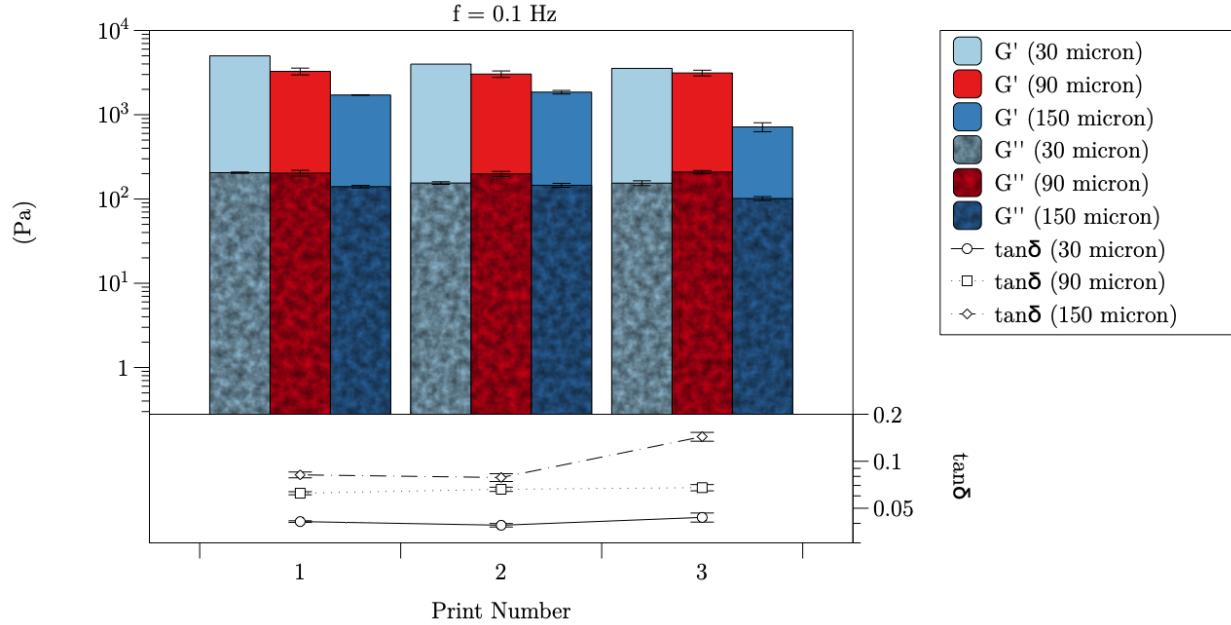


Figure 4: Primary axis: Storage Modulus at  $f = 0.1$  Hz with respect to print number for 30 micron, 90 micron, and 150 micron layer heights

Secondary axis:  $\tan \delta$  at  $f = 0.1$  Hz with respect to print number for 30 micron, 90 micron, and 150 micron layer heights

At  $f = 0.1$  Hz (4), the 30 micron prints show significant variation in storage modulus with respect to print 1. However,  $\tan \delta$  shows 5% difference for print 2 and 6% difference for print 3 with respect to print 1, implying the viscoelastic nature of the hydrogels printed at 30 microns may stay intact between resin iterations. This may have deeper significance, but must first be studied further. In comparison, the prints for 90 microns behave quite differently. The storage modulus varies by 7% at print 2 with respect to print 1, and by 4% at print 3 with respect to print 1. In addition,  $\tan \delta$  differs by 6% at print 2 and 8% at print 3, giving some promise of recycling potential. The 150 micron samples give similar promise at print 2: there is an 8% difference in storage modulus and 4% difference in  $\tan \delta$  with respect to print 1. However, there is once again significant variation in the third iteration of 150 micron samples, confirming that three iterations cannot be accomplished at 150 microns.

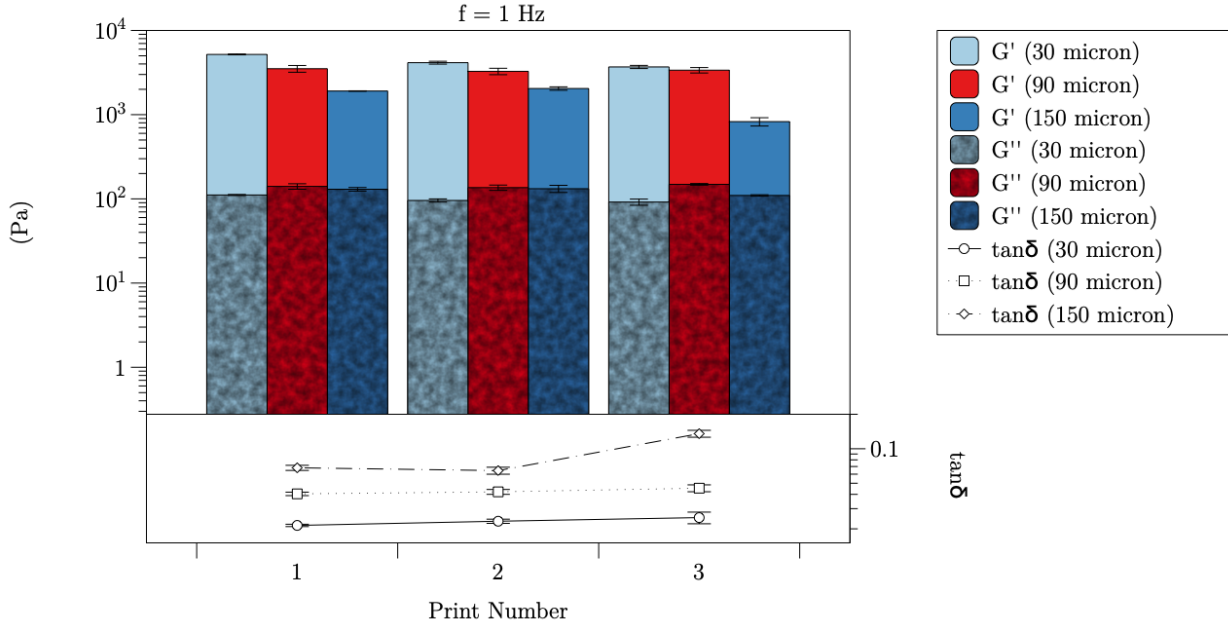


Figure 5: Primary axis: Storage Modulus at  $f = 1$  Hz with respect to print number for 30 micron, 90 micron, and 150 micron layer heights

Secondary axis:  $\tan \delta$  at  $f = 1$  Hz with respect to print number for 30 micron, 90 micron, and 150 micron layer heights

The 30 micron prints at  $f = 1$  (5) Hz vary enough to confirm they should only be printed with pristine resin. Furthermore, these results may provide insights into how the level of detail between layers impacts the resin quality post-print. However, the 90 micron prints exhibit storage modulus of 7% difference at print 2 and 4% difference at print 3, both with respect to print 1. Additionally,  $\tan \delta$  exhibits a 4% difference at print 2 and a 12% difference at print 3 with respect to print 1. Given the similar variations at  $f = 0.01$  Hz and  $f = 0.1$  Hz, we can see some promise in reusing resin for prints at 90 micron layer height. However, there is still enough variation between prints and within each respective print that more testing should be done before making any conclusions for this layer height. At 150 microns, the second resin iteration provided similar differences in storage modulus and  $\tan \delta$  with respect to print 1: 7% and 5%, respectively. In line with the results from  $f = 0.01$  Hz and  $f = 0.1$  Hz, the 150 micron hydrogels present similar viscoelastic characteristics between first and second iterations of the same resin. However, this is once again, a significant variation within the third resin iteration, leaving no hope for further recycling after the second iteration.

### 3.2 Photoinitiator Concentration

As per Protick et al., 2% TPO-Li photoinitiator, 10% acrylamide, and 0.3% bisacrylamide is a control resin for comparison with respect to a resin of similar monomer and crosslinker concentrations, but a TPO-Li concentration of 1.5% [protick]. Similar to the consecutive print analysis, we are reviewing frequencies:  $f = 0.01$  Hz 6,  $f = 0.1$  Hz 7, and  $f = 1$  Hz 8 due to the relevance with respect to biological tissue [lacoste, cheng, soetens, erisken]. For all three respective frequencies within the control resin, the storage modulus decreases far more than the loss modulus with increasing layer height. As a result, we see an increase in  $\tan \delta$  with respect to layer height, and thus an increase in viscous nature of the hydrogel as print detail decreases. Additionally, as the frequency increases, there is an overall decrease in  $\tan \delta$  for each respective layer height, signifying an overall trend towards elastic behavior with higher frequencies. Given that biological tissue typically express  $0.1 \leq \tan \delta \leq 0.2$  [protick], the control resin falls outside of that range with print details greater than 150 microns per layer with frequencies above 0.01 Hz. With this understanding, we can investigate how resins with 1.5% photoinitiator concentration compare, and if it is a viable resin substitute.

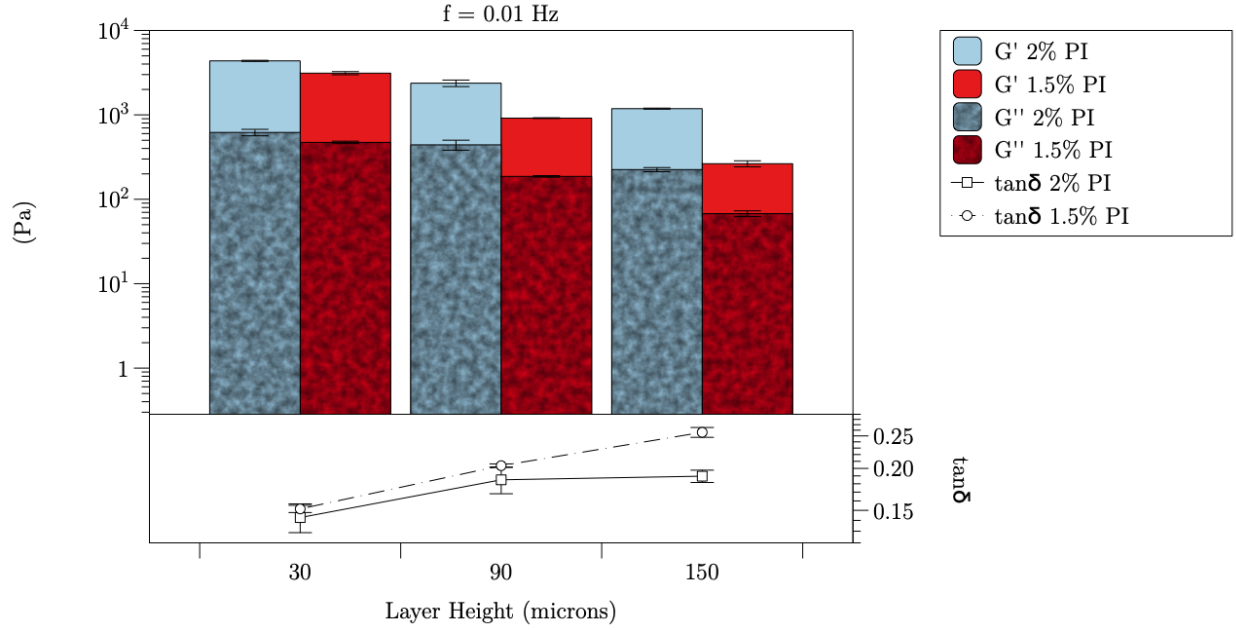


Figure 6: Primary axis: Storage Modulus at  $f = 0.01 \text{ Hz}$  with respect to layer height for 2% photoinitiator concentration and 1.5% photoinitiator concentration

Secondary axis:  $\tan \delta$  at  $f = 0.01 \text{ Hz}$  with respect to layer height for 2% photoinitiator concentration and 1.5% photoinitiator concentration

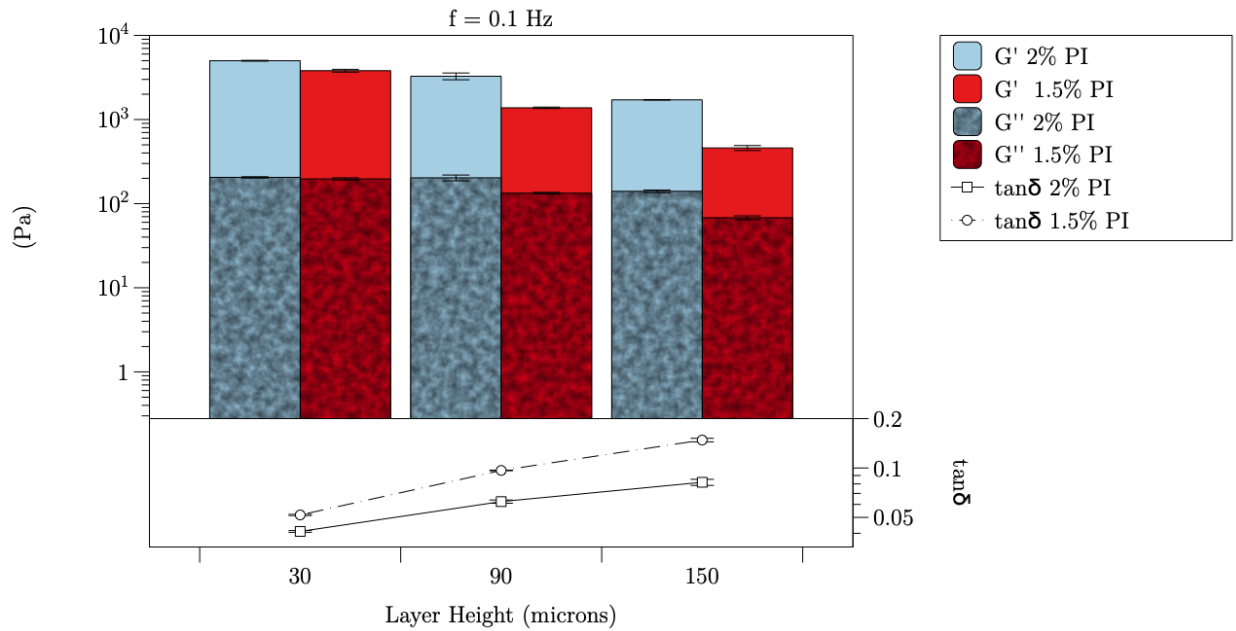


Figure 7: Primary axis: Storage Modulus at  $f = 0.1 \text{ Hz}$  with respect to layer height for 2% photoinitiator concentration and 1.5% photoinitiator concentration

Secondary axis:  $\tan \delta$  at  $f = 0.1 \text{ Hz}$  with respect to layer height for 2% photoinitiator concentration and 1.5% photoinitiator concentration

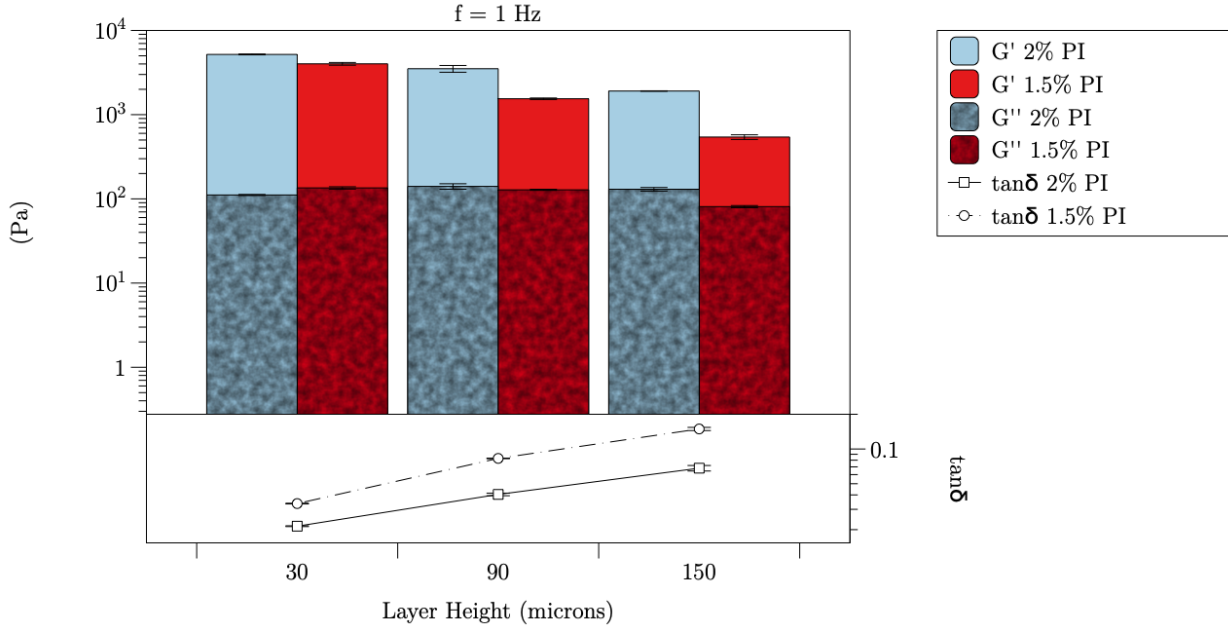


Figure 8: Primary axis: Storage Modulus at  $f = 1$  Hz with respect to layer height for 2% photoinitiator concentration and 1.5% photoinitiator concentration

Secondary axis:  $\tan \delta$  at  $f = 1$  Hz with respect to layer height for 2% photoinitiator concentration and 1.5% photoinitiator concentration

At  $f = 0.01$  Hz there is a noticeable difference in both storage modulus and loss modulus with respect to the control resin for all tested layer heights 6. Effectively, this already shows a lack of similarity between the resins, making it unusable as a substitute. Furthermore, we continue to see this trend at all layer heights for increasing frequencies. However, the 1.5% TPO-Li resin does show slightly more viscous properties at all layer heights with respect to the control resin, as  $(\tan \delta)_{1.5\%} > (\tan \delta)_{2\%}$  for all layer heights and frequencies. In fact, as the frequency increases, the hydrogels produced with 1.5% TPO-Li are much closer to the  $\tan \delta$  range for biological tissue [protick] — this is especially true of prints with 90 micron layer height. Although 1.5% TPO-Li resin may not be used as a replacement for 2% TPO-Li resin, it may be a viable alternative due to the rheological properties that it presents. To test this theory, it will be important to continue testing, and to begin the process of checking for biological compatibility. Furthermore, this finding gives hope for finding alternative concentrations that provide superior properties.

## 4 Conclusion

We are trending away from mass-produced goods and towards a world filled with individualized pieces that fit our unique and specific needs. Additive manufacturing is the bridge that continues to lead us toward this reality. As our understanding of material properties continues to grow, so will our ability to harness those properties to optimize our world and each other. An important path we continue to forge is in biomaterials, whose properties are difficult to harness, and result in material waste — exactly what we are trying to reduce with additive manufacturing.

Ultimately, there is still much work needed to be done before resin recycling can become a reality. The hydrogels exhibit complex variations between print iterations, making it difficult to predict how they will behave in subsequent resin iterations. However, we have seen promise in both 90 micron and 150 micron layer height samples for second iterations of resin — this not only opens up the possibility for further resin recycling, but also for further investigation into how layer height can influence the resin quality after a print. Furthermore, we saw small differences in  $\tan \delta$  between iterations for all layer heights, implying the

viscoelastic nature of the hydrogels is somewhat maintained between print iterations. It will be important to investigate this phenomenon further to better understand the mechanisms that influence mechanical biocompatibility within hydrogels.

Additionally, our work in photoinitiator variation led us to uncover alternative resin makeups that may produce superior hydrogels. We followed a recipe that produced acceptable results, though it also resulted in less-than favorable mechanical properties. Our reduced TPO-Li resin provided a theoretically more favorable  $\tan \delta$ , though it did not mimic the tested properties of the control resin. In turn, we may have glimpsed into the greater possibilities that come with changing resin makeup – we need to continue varying concentrations to find optimal concentrations. However, this will result in more testing, and more waste. So, in conjunction with testing resins, it will be important to figure out whether consecutive printing will be a viable option. Additionally, our work will open up possibilities for modeling and other theoretical work that can reduce waste.

## 5 Acknowledgements

We would like to thank Dr. Sabrina Nilufar for her insights and laboratory equipment. We also thank Dr. Farhan Chowdhury for his laboratory equipment. Additionally, we thank Dr. Boyd Goodson and Dr. Saikat Talapatra for their work in facilitating the Southern Illinois University at Carbondale NSF Summer REU. Finally, we thank the National Science Foundation Grant: #.